Malaysian Journal of Mathematical Sciences 17(1): 1–12 (2023)
https://doi.org/10.47836/mjms.17.1.01

Malaysian Journal of Mathematical Sciences

Journal homepage: https://mjms.upm.edu.my

On the Solution of a Nonlinear Fractional-Order Glucose-Insulin System Incorporating β-cells Compartment

Ahmad Alalyani *

Department of Mathematics, Faculty of Science and Arts in Almandaq, Al-Baha University, Saudi Arabia

E-mail: azaher@bu.edu.sa
**Corresponding author*

Received: 12 May 2022
Accepted: 29 September 2022

Abstract

In this work, we are interested in studying variations in plasma glucose and insulin levels over time using a fractional-order version of a mathematical model. Applying the fractional-order Caputo derivative, we can investigate different concentration rates among insulin, glucose, and healthy β-cells. The main aim is to obtain the numerical solution of the proposed model in order to show variations in plasma glucose and insulin levels over time, by applying the generalized Euler method. The local stability analysis of the proposed (discretization) Caputo fractional-order model was discussed. To check the feasibility of our analysis, we have investigated some numerical simulations for various fractional orders by varying values of the parameters with help of Mathematica. Numerical simulations were in good agreement with the theoretical findings. Three specific numerical examples are given as applications of the main results.

Keywords: nonlinear fractional-order model; glucose-insulin system; β-cells kinetics; generalized Euler method.

1 Introduction

The fractional calculus is the calculus of non-integer order, which is a generalization of integral and differential integer-order calculus. Fractional calculus was initially applied by Abel [1] in his answer to the Tautochrone problem. Therefore, it is mostly applied in physics, biology, medicine, viscoelasticity, bioengineering, economics, and control theory, and it would be too long to list all the research dealing with that. For instance, the reader can refer to [4, 10, 12] and references therein, among others.

It is well known that mathematical models are an excellent option to study and predict natural phenomena to some extent. In this way, fractional-order theory gives us a framework to add memory properties and an additional dimension to the mathematical models in order to more accurately approximate real-world phenomena. Numerous diverse metabolic issues can arise, such as type I and type II diabetes, hyperinsulinemia, hypoglycemia, etc., in the human glucose-insulin regulation system. Therefore, it is essential to characterize and analyze such a biological system. Thus, the analysis and characterization of such a biological system are a must. The fractional-order operator provides improved accuracy of the underlying glucose-insulin disorders.

Stability analysis is an important technique for the analysis of mathematical models. It shows how mathematical models respond to modifications. The use of stability analysis is required to have information on both the stability of solutions to differential equations and the stability of dynamical systems. Several novel and significant advances have been made in stability analysis and analytical solutions for differential equations (see, for example, but not limited to, [3, 20, 21]).

There is a voluminous literature that uses mathematical models to deal with the dynamics of the connection between glucose and the hormone that controls it, insulin. Some of the papers are [6, 9, 17]. In 1971, Atkins in [7] noted that such mathematical models had one or more flaws. Those flaws were the lack of some of the desired data, the fact that it is very complicated to study the model for a small amount of used data, the experiment's time frame is too short, and the models are not compatible with existing data. Furthermore, there are no simulations that were carried out to examine the mathematical model. In 1987, Bajaj et al. [8] proposed the following model:

$$
\begin{aligned}
\frac{dx}{dt} &= R_1 y - R_2 x + c_1, \\
\frac{dy}{dt} &= \frac{R_3 N}{z} - R_4 x + c_2, \\
\frac{dz}{dt} &= R_5 y(T - z) + R_6 z(T - z) - R_7 z.
\end{aligned} \tag{1}
$$

Bajaj et al. developed and numerically discussed the model (1) in [8]. They used the Runge-Kutta-Merson integration scheme to numerically solve the set of three nonlinear coupled ordinary differential equations (1).

This work considers a nonlinear fractional-order (glucose-insulin-β-cells) model with a nonlinear incidence rate in the sense of the Caputo derivative $\frac{d^\nu}{dt^\nu}$ and is given by

$$
\begin{aligned}
\frac{d^\nu x}{dt^\nu} &= R_1 y - R_2 x + c_1, \\
\frac{d^\nu y}{dt^\nu} &= \frac{R_3 N}{z} - R_4 x + c_2, \\
\frac{d^\nu z}{dt^\nu} &= R_5 y(T - z) + R_6 z(T - z) - R_7 z,
\end{aligned} \tag{2}
$$

with the initial conditions

$$x(0) = x_0, y(0) = y_0, z(0) = z_0,$$

where R_1 is the rate at which insulin concentration increases due to blood glucose increase, R_2 is the rate at which insulin is reduced, R_3 is the rate at which β-cells are lost, R_4 is the decrease rate of glucose in response to insulin production, R_5 is the increase rate in dividing β-cells due to interaction between them and blood glucose, R_6 is the rate of increase in β-cells due to dividing and non-dividing them, R_7 is the rate of decrease in β-cells due to its current level, N is a constant, c_1 and c_2 are the constant rates of increase in x and y, respectively, the total number of dividing and non-dividing is represented by T, the plasma insulin concentrations are represented by x, the plasma glucose concentrations are represented by y, and the β-cells density in the proliferative phase is represented by z.

The contribution of this study is to show that fractional order modeling outperforms integer order modeling. According to [5], the existence, uniqueness, nonegativity, and boundedness of the solution to the equation (2) have all been studied. The global stability of the infection-free and endemic equilibrium point of the proposed model has been fully established using the Lyapunov-LaSalle type theorem. The analysis of the local stability of the discretization model is discussed. Further, the numerical solution of the model (2) is obtained by applying the generalized Euler discretization method in order to describe the changes in time of plasma glucose and insulin levels. Moreover, some numerical results and simulations for three different test problems are discussed. Our strategy relies on applying the generalized Euler discretization method that was established by Odibat and Momani in [14]. The model is also developed using a numerical algorithm, and the results of a computational experiment are presented. Applications of the suggested method are also discussed, with the proposed and modified methods producing impressive results. Using the suggested methodologies, the numerical solutions to the model (2) are in good agreement with the analytical solutions. We can infer that the suggested approaches, which were derived or changed in this research, are quite effective based on the numerical results produced utilizing the provided methods. The results of this manuscript could potentially complement the literature on this subject (see, for example, but not limited to, [2, 18, 19]).

The structure of this article is as follows: Section 2 describes the application of the generalized Euler discretization method and discusses the analysis of the local stability of the discretization model. Section 3 gives some numerical results and simulations for three different test problems. Section 4 presents our conclusions.

2 Generalized Euler Method (See [14])

Recall that $\dfrac{d^\nu}{dt^\nu}$ is called the Caputo fractional derivative of order ν and is defined in [16] as: For $\nu > 0, n-1 < \nu < n, n \in \mathbb{N}$,

$$\frac{d^\nu}{dt^\nu} = \begin{cases} \dfrac{1}{\delta(n-\nu)} \displaystyle\int_0^t \frac{f^{(n)}(s)}{(t-s)^{\nu+1-n}}\, ds, & n-1 < \nu < n, \\ \dfrac{d^n}{dt^n} f, & \nu = n. \end{cases}$$

To investigate the numerical solution of the model (2), we use in this section the generalized Euler discretaization approach, that was established by Odibat and Momani (see [14]). Let us start by writing the Caputo fractional-order model (2) in the following system form:

$$\mathcal{D}^\nu M = F(M), \quad t \in [0, T], \quad 0 < \nu \leq 1, \quad M(0) = M_0, \tag{3}$$

where

$$M = \begin{bmatrix} x \\ y \\ z \end{bmatrix}, \quad M_0 = \begin{bmatrix} x_0 \\ y_0 \\ z_0 \end{bmatrix}, \quad F(M) = \begin{bmatrix} R_1 y - R_2 x + c_1 \\ \frac{R_3 N}{z} - R_4 x + c_2 \\ R_5 y(T-z) + R_6 z(T-z) - R_7 z \end{bmatrix}.$$

The generalized Euler formula for the model (2) is given by the following proposition.

Prop 2.1. *Let $[0, a]$ be the interval for the solution of the model (2). The general formula for the generalized Euler method of (2) is provided by:*

$$\begin{aligned} x(t_{j+1}) &= x(t_j) + \frac{h^\nu}{\Gamma(\nu+1)} \left[R_1 y(t_j) - R_2 x(t_j) + c_1 \right], \\ y(t_{j+1}) &= y(t_j) + \frac{h^\nu}{\Gamma(\nu+1)} \left[\frac{R_3 N}{z(t_j)} - R_4 x(t_j) + c_2 \right], \\ z(t_{j+1}) &= z(t_j) + \frac{h^\nu}{\Gamma(\nu+1)} [R_5 y(t_j)(T - z(t_j)) + R_6 z(t_j)(T - z(t_j)) - R_7 z(t_j)], \end{aligned} \tag{4}$$

where the Euler gamma function Γ is defined as:

$$\Gamma(z) = \int_s^\infty e^{-t} t^{z-1} dt, \; t > 0$$

and $h = \frac{a}{k}$ is the step size in the sub-intervals $[t_j, t_{j+1}]$ of the interval $[0, a]$.

Proof. Consider the following initial value problem:

$$\begin{aligned} \frac{d^\nu x(t)}{dt^\nu} &= f_1(t, x, y, z) = R_1 y(t) - R_2 x(t) + c_1, \\ \frac{d^\nu y(t)}{dt^\nu} &= f_2(t, x, y, z)) = \frac{R_3 N}{z(t)} - R_4 x(t) + c_2, \\ \frac{d^\nu z(t)}{dt^\nu} &= f_3(t, x, y, z) = R_5 y(t)(T - z(t)) + R_6 z(t)(T - z(t)) - R_7 z(t), \end{aligned} \tag{5}$$

for $t \in [0, T]$, $0 < \alpha \leq 1$, using the initial conditions

$$x(0) = x_0, y(0) = y_0, z(0) = z_0.$$

We need to produce a collection of $\{(t_j, f(t_j))\}$ points and use the points for our approximation. Let $[0, a]$ be the interval over which the solution of (5) is to be discussed. The $[0, a]$ interval is subdivided into k sub-intervals $[t_j, t_{j+1}]$ of the same width $h = \frac{a}{k}$ by using the $t_j = jh$ nodes, where $j = 0, 1, \cdots, k$. Assume that x, y, z, $\mathcal{D}^\nu x$, $\mathcal{D}^\nu y$, $\mathcal{D}^\nu z$, $\mathcal{D}^{2\nu} x$, $\mathcal{D}^{2\nu} y$ and $\mathcal{D}^{2\nu} z$ are continuous in $[0, a]$, and use Taylor's generalized formula in [13] to extend y to $t = t_s = 0$. Thus, there is a value c_1 for each value t, so that

$$\begin{aligned} x(t) &= x(t_s) + (\mathcal{D}^\nu x(t))(t_s) \frac{t^\nu}{\Gamma(\nu+1)} + (\mathcal{D}^{2\nu} x(t))(c_1) \frac{t^{2\nu}}{\Gamma(2\nu+1)} \\ y(t) &= y(t_s) + (\mathcal{D}^\nu y(t))(t_s) \frac{t^\nu}{\Gamma(\nu+1)} + (\mathcal{D}^{2\nu} y(t))(c_1) \frac{t^{2\nu}}{\Gamma(2\nu+1)} \\ z(t) &= z(t_s) + (\mathcal{D}^\nu z(t))(t_s) \frac{t^\nu}{\Gamma(\nu+1)} + (\mathcal{D}^{2\nu} z(t))(c_1) \frac{t^{2\nu}}{\Gamma(2\nu+1)}. \end{aligned} \tag{6}$$

When $(\mathcal{D}^{\nu}\, x(t))(t_s) = f_1(t_s, x(t_s), y(t_s), z(t_s))$, $(\mathcal{D}^{\nu}\, y(t))(t_s) = f_2(t_s, x(t_s), y(t_s), z(t_s))$, $(\mathcal{D}^{\nu}\, z(t))(t_s) = f_3(t_s, x(t_s), y(t_s), z(t_s))$, and $h = t$ are substituted into (6), then we get

$$\begin{aligned} x(t_1) &= x(t_s) + f_1(t_s, x(t_s), y(t_s), z(t_s))\frac{h^{\nu}}{\Gamma(\nu+1)} + (\mathcal{D}^{2\nu}\, x(t))(c_1)\frac{h^{2\nu}}{\Gamma(2\nu+1)} \\ y(t_1) &= y(t_s) + f_2(t_s, x(t_s), y(t_s), z(t_s))\frac{h^{\nu}}{\Gamma(\nu+1)} + (\mathcal{D}^{2\nu}\, y(t))(c_1)\frac{h^{2\nu}}{\Gamma(2\nu+1)} \\ z(t_1) &= z(t_s) + f_3(t_s, x(t_s), y(t_s), z(t_s))\frac{h^{\nu}}{\Gamma(\nu+1)} + (\mathcal{D}^{2\nu}\, z(t))(c_1)\frac{h^{2\nu}}{\Gamma(2\nu+1)}. \end{aligned} \tag{7}$$

The second-order term (including $h^{2\nu}$) may be ignored if the h step size is small enough, and we will obtain it.
The discrete form of (5) can be defined in terms of (7) as follows:

$$\begin{aligned} x(t_1) &= x(t_s) + m\left[R_1 y(t_s) - R_2 x(t_s) + c_1\right], \\ y(t_1) &= y(t_s) + m\left[\frac{R_3 N}{z(t_s)} - R_4 x(t_s) + c_2\right], \\ z(t_1) &= z(t_s) + m[R_5 y(t_s)(T - z(t_s)) + R_6 z(t_s)(T - z(t_s)) - R_7 z(t_s)], \end{aligned} \tag{8}$$

where $m = \dfrac{h^{\nu}}{\Gamma(\nu+1)}$.
The method is repeated until a point sequence that approximates the solution is obtained.
Hence, when $t_{j+1} = t_j + h$, (4) is obtained.
When $j = 0, 1, \cdots, -k-1$, (4) is obviously reduced to the classical Euler scheme when $\nu = 1$. □

2.1 Stability Analysis of a Discretization Model

In this subsection, the local stability of the discretization model will be analyzed in sense of the general formula for the generalized Euler method (4).

Lemma 2.1. *Consider the equilibrium point $\bar{E} = (x_s, y_s, z_s)$, where the steady-state values x_s and y_s are provided by:*

$$x_s = \frac{R_4 N + c_1 z_s}{R_5 z_s}, \qquad y_s = \frac{R_4 R_7 N + (R_7 c_1 - R_5 c_2) z_s}{R_5 R_6 z_s}$$

and z_s satisfies

$$z_s^3 + q_1 z_s^2 + q_2 z_s + q_3 = 0,$$

where

$$\begin{aligned} q_1 &= \frac{(R_3 c_1 - T R_2 c_1 + R_7 c_1 - R_5 c_2) R_1}{R_2 R_5 R_6}, \\ q_2 &= \frac{(R_4 R_7 N - T R_7 c_1 + T R_5 c_2) R_1}{R_2 R_5 R_6}, \\ q_3 &= \frac{T R_1 R_4 R_7 N}{R_2 R_5 R_6}. \end{aligned}$$

Then, $\bar{E}$ is locally asymptotically stable.

Proof. The Jacobian matrix $J(\bar{E})$ of the model (4) is given by:

$$J(\bar{E}) = \begin{bmatrix} 1 - mR_2 & mR_1 & 0 \\ -mR_4 & 1 & \dfrac{-mR_3 N}{z_s^2} \\ 0 & mR_5(T - z_s) & 1 - m(R_5 y_s - R_6 T + 2R_6 z_s + R_7) \end{bmatrix}. \tag{9}$$

The characteristic polynomial of (9) is:

$$P(\lambda) = \beta_0\lambda^3 + \beta_1\lambda^2 + \beta_2\lambda + \beta_3 = 0, \tag{10}$$

where

$$\begin{aligned}
\beta_0 &= 1,\\
\beta_1 &= -3 + m(R_2 + R_7 + R_5y_s - R_6T + 2R_6z_s),\\
\beta_2 &= 3 - m(2R_2 + 2R_7 + 2R_5y_s - 2R_6T + 4R_6z_s)\\
&\quad + m^2\left(R_1R_4 + R_2R_7 - R_2R_6T + R_2R_5y_s + 2R_2R_6z_s + \frac{R_3R_5N(T - z_s)}{z_s^2}\right),\\
\beta_3 &= -1 + m(R_2 + R_7 + R_5y_s - R_6T + 2R_6z_s)\\
&\quad - m^2\left(R_1R_4 + R_2R_7 - R_2R_6T + R_2R_5y_s + 2R_2R_6z_s + \frac{R_3R_5N(T - z_s)}{z_s^2}\right)\\
&\quad + m^3\left(R_1R_4R_7 - R_1R_4R_6T + R_1R_4R_5y_s + 2R_1R_4R_6z_s + \frac{R_2R_3R_5N(T - z_s)}{z_s^2}\right).
\end{aligned}$$

Let us mention that the Routh-Hurwitz Array for (9) is:

$$D(\bar{E}) = -\begin{vmatrix} \beta_3 & \beta_1 \\ \beta_2 & \beta_0 \\ \dfrac{(\beta_1\beta_2 - \beta_0\beta_3)}{\beta_2} & 0 \\ \beta_0 & 0 \end{vmatrix}.$$

According to the Routh-Hurwitz conditions [11], confirming that $\dfrac{(\beta_1\beta_2 - \beta_0\beta_3)}{\beta_2}$ has the same sign with β_1, then the three eigenvalues have negative real parts. Since

$$\beta_0 > 0, \beta_1 > 0, \beta_2 > 0, \beta_3 > 0, \frac{(\beta_1\beta_2 - \beta_0\beta_3)}{\beta_2} > 0 \text{ and } \beta_1\beta_2 > \beta_0\beta_3$$

hold, then the Routh-Hurwitz stability criterions are satisfied, and $\bar{E}$ is locally asymptotically stable. □

3 Numerical Results and Simulations

In this section, we give some numerical outputs and simulations for each of the 3 different test problems. The generalized Euler discretization method was used to obtain the numerical outputs and simulations.

Consider the following model

$$\begin{aligned}
x(t_{j+1}) &= x(t_j) + m\Big[0.79196\, y(t_j) - 0.24537\, x(t_j) + 0.37538\Big],\\
y(t_{j+1}) &= y(t_j) + m\Big[\frac{9.52033\,(1.4)}{z(t_j)} - 2.84575\, x(t_j) + 1.03482\Big],\\
z(t_{j+1}) &= z(t_j) + m\Big[0.02139\, y(t_j)(1.95 - z(t_j)) + 0.02747 z(t_j)(1.95 - z(t_j)) - 0.18311\, z(t_j)\Big],
\end{aligned} \tag{11}$$

subject to the initial conditions

$$\Big(x(0), y(0), z(0)\Big) = \Big(6.03502, 1.79015, 0.825837\Big).$$

Table 1: Some Numerical outputs of (x, y, z) for Example 1.

(x,y,z)	(x,y,z)	(x,y,z)
$\nu = 0.8$	$\nu = 0.95$	$\nu = 1$
(6.04344 , 1.79015 , 0.823607)	(6.03903 , 1.79015 , 0.824775)	(6.03814 , 1.79015 , 0.82501)
(6.05181 , 1.79068 , 0.821391)	(6.04303 , 1.79027 , 0.823716)	(6.04126 , 1.79022 , 0.824185)
(6.06013 , 1.79175 , 0.819187)	(6.04702 , 1.79051 , 0.822659)	(6.04437 , 1.79037 , 0.823362)
(6.06842 , 1.79336 , 0.816997)	(6.051 , 1.79087 , 0.821606)	(6.04747 , 1.79059 , 0.822541)
(6.07669 , 1.7955 , 0.81482)	(6.05497 , 1.79136 , 0.820556)	(6.05056 , 1.79088 , 0.821721)
(6.08495 , 1.79819 , 0.812657)	(6.05893 , 1.79196 , 0.819508)	(6.05365 , 1.79125 , 0.820903)
(6.09322 , 1.80142 , 0.810508)	(6.06288 , 1.79269 , 0.818464)	(6.05674 , 1.79169 , 0.820088)
(6.10149 , 1.80518 , 0.808374)	(6.06683 , 1.79354 , 0.817423)	(6.05982 , 1.7922 , 0.819273)
(6.1098 , 1.80948 , 0.806255)	(6.07078 , 1.79451 , 0.816385)	(6.0629 , 1.79279 , 0.818461)
(6.11814 , 1.81432 , 0.80415)	(6.07473 , 1.7956 , 0.81535)	(6.06598 , 1.79345 , 0.817651)

For the parameters of the model (11), we chose different values of $\nu = \{0.8, 0.95, 1\}$. Figures (1(a)-1(c)) show the dynamical behavior of $x(t)$, $y(t)$ and $z(t)$ for various values of $\nu = \{0.8, 0.95, 1\}$ for the parameters of (11). Figures (2(a)-2(c)) show the behavior of $x(t)$, $y(t)$ and $z(t)$ versus time using various values of $\nu = \{0.8, 0.95, 1\}$ for the parameters of (11). By Lemma 2.1, $\bar{E}$ is asymptotically stable for the parameters of the model (11), and the solution of (11) converges to $\bar{E}$.

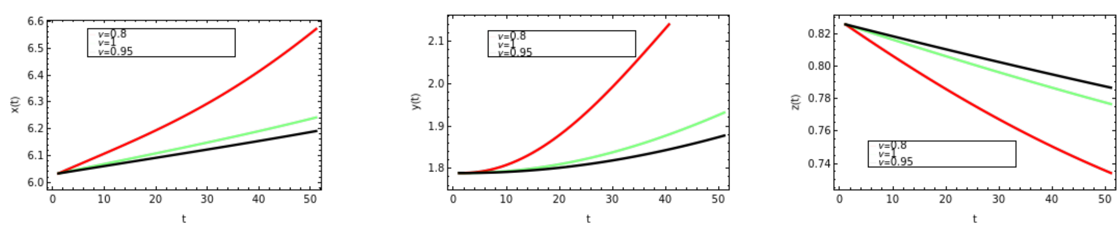

(a) (b) (c)

Figure 1: The dynamical behavior of $x(t)$, $y(t)$ and $z(t)$ using different values of $\nu = \{0.8, 0.95, 1\}$ for the parameters existed in Example 1.

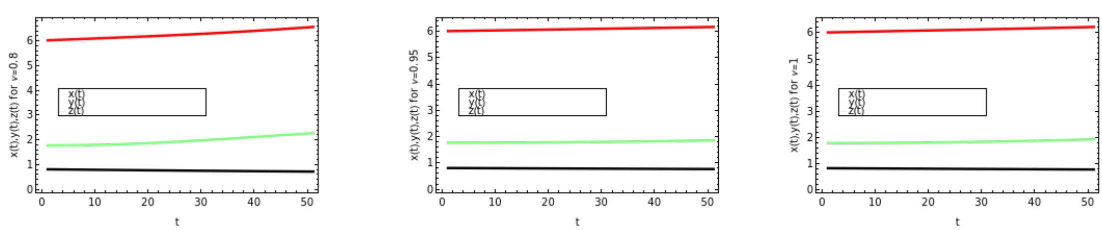

(a) (b) (c)

Figure 2: $x(t)$, $y(t)$ and $z(t)$ versus time using different values of $\nu = \{0.8, 0.95, 1\}$ for the parameters existed in Example 1.

Consider the following model

$$
\begin{aligned}
x(t_{j+1}) &= x(t_j) + m\Big[0.472\, y(t_j) - 0.25\, x(t_j) + 0.1\Big],\\
y(t_{j+1}) &= y(t_j) + m\Big[\frac{0.82(1.27)}{z(t_j)} - 0.6\, x(t_j) + 0.8\Big],\\
z(t_{j+1}) &= z(t_j) + m\Big[0.3\, y(t_j)(1.5 - z(t_j)) + 0.3\, z(t_j)(1.5 - z(t_j)) - 0.2\, z(t_j)\Big],
\end{aligned} \tag{12}
$$

using the initial conditions

$$\Big(x(0), y(0), z(0)\Big) = \Big(6.03502, 1.79015, 0.825837\Big).$$

Table 2: Some Numerical outputs of (x, y, z) for Example 2.

(x, y, z)	(x, y, z)	(x, y, z)
$\nu = 0.8$	$\nu = 0.95$	$\nu = 1$
(6.01981 , 1.74808 , 0.835652)	(6.02778 , 1.77011 , 0.830512)	(6.02938 , 1.77455 , 0.829476)
(6.00418 , 1.70585 , 0.845032)	(6.02043 , 1.75003 , 0.835089)	(6.02368 , 1.75893 , 0.833055)
(5.98811 , 1.66351 , 0.853992)	(6.01299 , 1.72992 , 0.839568)	(6.01793 , 1.74329 , 0.836575)
(5.9716 , 1.62107 , 0.862544)	(6.00546 , 1.70978 , 0.843952)	(6.01211 , 1.72763 , 0.840037)
(5.95467 , 1.57858 , 0.870701)	(5.99782 , 1.68962 , 0.848241)	(6.00623 , 1.71195 , 0.84344)
(5.93732 , 1.53606 , 0.878475)	(5.99009 , 1.66944 , 0.852436)	(6.0003 , 1.69626 , 0.846787)
(5.91954 , 1.49353 , 0.885878)	(5.98226 , 1.64924 , 0.85654)	(5.99431 , 1.68056 , 0.850077)
(5.90133 , 1.45102 , 0.892923)	(5.97433 , 1.62902 , 0.860554)	(5.98825 , 1.66484 , 0.853311)
(5.88271 , 1.40856 , 0.899619)	(5.9663 , 1.60879 , 0.864479)	(5.98214 , 1.64912 , 0.85649)
(5.86368 , 1.36616 , 0.905979)	(5.95818 , 1.58855 , 0.868316)	(5.97597 , 1.63338 , 0.859614)

For the parameters of the model (12), we chose different values of $\nu = \{0.8, 0.95, 1\}$. Figures (3(a)-3(c)) show the dynamical behavior of $x(t)$, $y(t)$ and $z(t)$ for various values of $\nu = \{0.8, 0.95, 1\}$ for the parameters of (12). Figures (4(a)-4(c)) show the behavior of $x(t)$, $y(t)$ and $z(t)$ versus time using various values of $\nu = \{0.8, 0.95, 1\}$ for the parameters of (12). By Lemma 2.1, $\bar{E}$ is asymptotically stable for the parameters of the model (12), and the solution of (12) converges to $\bar{E}$.

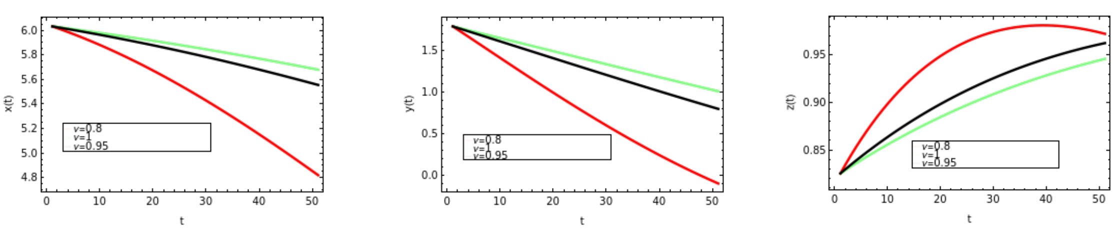

(a) (b) (c)

Figure 3: The dynamical behavior of $x(t)$, $y(t)$ and $z(t)$ using different values of $\nu = \{0.8, 0.95, 1\}$ for the parameters existed in Example 2.

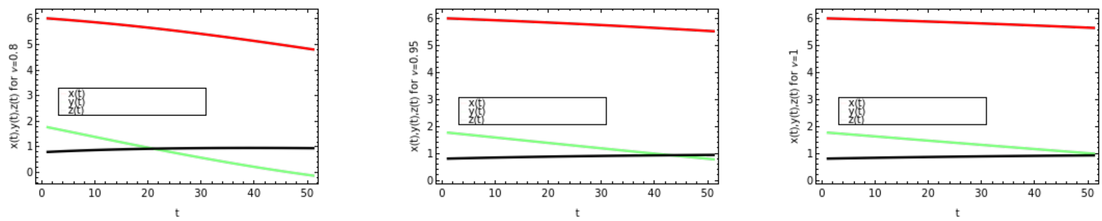

(a) (b) (c)

Figure 4: $x(t)$, $y(t)$ and $z(t)$ versus time using different values of $\nu = \{0.8, 0.95, 1\}$ for the parameters existed in Example 2.

Consider the following model

$$\begin{aligned}
x(t_{j+1}) &= x(t_j) + m\Big[0.865\, y(t_j) - 0.268\, x(t_j) + 0.41\Big],\\
y(t_{j+1}) &= y(t_j) + m\Big[\frac{0.736}{z(t_j)} - 0.22\, x(t_j) + 0.08\Big],\\
z(t_{j+1}) &= z(t_j) + m\Big[0.33\, y(t_j)\,(1000 - z(t_j)) + 0.03\, z(t_j)\,(1000 - z(t_j)) - 0.2\, z(t_j)\Big],
\end{aligned} \tag{13}$$

using the initial conditions

$$\Big(x(0), y(0), z(0)\Big) = \Big(6.03502, 1.79015, 0.825837\Big).$$

Table 3: Some Numerical outputs of (x, y, z) for Example 3.

(x, y, z)	(x, y, z)	(x, y, z)
$\nu = 0.8$	$\nu = 0.95$	$\nu = 1$
(6.04422 , 1.79015 , 0.840044)	(6.0394 , 1.79015 , 0.832605)	(6.03843 , 1.79015 , 0.831105)
(6.05335 , 1.78953 , 0.853951)	(6.04377 , 1.79001 , 0.839305)	(6.04183 , 1.79006 , 0.836331)
(6.0624 , 1.78831 , 0.867559)	(6.04812 , 1.78973 , 0.845937)	(6.04522 , 1.78989 , 0.841517)
(6.07136 , 1.78653 , 0.880867)	(6.05245 , 1.78931 , 0.852501)	(6.04861 , 1.78964 , 0.846661)
(6.08021 , 1.78421 , 0.893877)	(6.05677 , 1.78876 , 0.858997)	(6.05198 , 1.7893 , 0.851764)
(6.08895 , 1.78138 , 0.90659)	(6.06106 , 1.78808 , 0.865425)	(6.05533 , 1.78888 , 0.856826)
(6.09755 , 1.77806 , 0.919007)	(6.06533 , 1.78727 , 0.871785)	(6.05868 , 1.78839 , 0.861847)
(6.10602 , 1.77428 , 0.931132)	(6.06957 , 1.78634 , 0.878077)	(6.06201 , 1.78781 , 0.866826)
(6.11433 , 1.77006 , 0.942966)	(6.07379 , 1.78529 , 0.884302)	(6.06533 , 1.78716 , 0.871765)
(6.12249 , 1.7654 , 0.954512)	(6.07799 , 1.78412 , 0.89046)	(6.06863 , 1.78644 , 0.876662)

For the parameters of the model (13), we chose different values of $\nu = \{0.8, 0.95, 1\}$. Figures (5(a)-5(c)) show the dynamical behavior of $x(t)$, $y(t)$ and $z(t)$ for various values of $\nu = \{0.8, 0.95, 1\}$ for the parameters of (13). Figures (6(a)-6(c)) show the behavior of $x(t)$, $y(t)$ and $z(t)$ versus time using various values of $\nu = \{0.8, 0.95, 1\}$ for the parameters of (13). By Lemma 2.1, $\bar{E}$ is asymptotically stable for the parameters of the model (13), and the solution of (13) converges to $\bar{E}$.

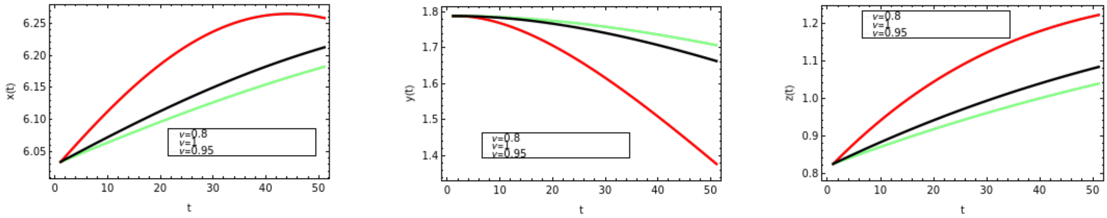

(a) (b) (c)

Figure 5: The dynamical behavior of $x(t)$, $y(t)$ and $z(t)$ using different values of $\nu = \{0.8, 0.95, 1\}$ for the parameters existed in Example 3.

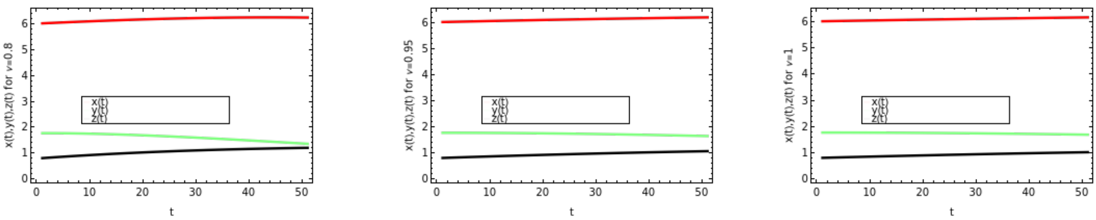

(a) (b) (c)

Figure 6: $x(t)$, $y(t)$ and $z(t)$ versus time using different values of $\nu = \{0.8, 0.95, 1\}$ for the parameters existed in Example 3.

4 Conclusions

In this paper, we have presented the Caputo fractional-order model (2) and its discretized model (4) that describes the concentration rates among insulin, glucose, and healthy β-cells. The analysis of the local stability of the presented (discretization) Caputo fractional-order model has been discussed. Further, we have computed numerical solutions for the considered model via a powerful technique due to Euler. For the demonstration of our proposed method, we provide graphical representation of the concerned results using some real values for the parameters involve in our considered model. Here, we have derived an algorithm to simulate our results for the considered nonlinear systems. The numerical solution of the proposed model (4) shows time efficiency on $x(t)$, $y(t)$ and $z(t)$ concentrations. Numerical simulation is done by using the generalized Euler method. From the numerical simulations, it is deduced that the dynamical behaviors for the levels of $x(t)$, $y(t)$ and $z(t)$ are stable over time. On the basis of numerical results and simulations, it is concluded that the proposed model is stable at the equilibrium point $\bar{E}$ and is better than its integer order form. In future work, we will investigate a control scheme to drive the glucose-insulin system to stable behavior. Researchers from many scientific areas can also extend this work to other biological systems.

Data Availability The experimental data used to support the findings of this study are taken from [15].

Acknowledgement We are thankful to anonymous reviewers for their valuable comments and suggestions to improve the presentation of this paper.

Conflicts of Interest The author declares that he has no conflicts of interest to report regarding the publication of this study.

References

[1] N. H. Abel (1823). Solution de quelques problèmes à l'aide d'intégrales définies. *Mag. Naturv.*, *1*(2), 1–127.

[2] E. Ackerman, J. W. Rosevear & W. F. McGuckin (1964). A mathematical model of the glucose-tolerance test. *Phys. Med. Biol.*, *9*(2), 203–213. https://doi.org/10.1088/0031-9155/9/2/307.

[3] N. A. Ahmad, N. Senu, Z. B. Ibrahim & M. Othman (2022). Stability analysis of diagonally implicit two derivative runge-kutta methods for solving delay differential equations. *Malaysian Journal of Mathematical Sciences*, *16*(2), 215–235. https://doi.org/10.47836/mjms.16.2.04.

[4] S. M. Al-Zahrani, F. E. I. Elsmih, K. S. Al-Zahrani & S. Saber (2022). A fractional order SITR model for forecasting of transmission of COVID-19: sensitivity statistical analysis. *Malaysian Journal of Mathematical Sciences*, *16*(3), 517–536. https://doi.org/10.47836/mjms.16.3.08.

[5] A. Alalyani (2022). Numerical solution of the fractional-order mathematical model of β-cells kinetics and glucose-insulin system using a predictor corrector method. *Mathematical Models and Computer Simulations*, *14*(1), 159–171. https://doi.org/10.1134/S2070048222010021.

[6] M. H. Alshehri, S. Saber & F. Z. Duraihem (2021). Dynamical analysis of fractional-order of IVGTT glucose-insulin interaction. *International Journal of Nonlinear Sciences and Numerical Simulation*, pp. 000010151520200201. https://doi.org/10.1515/ijnsns-2020-0201.

[7] G. L. Atkins (1971). Investigation of some theoretical models relating the concentrations of glucose and insulin in plasma. *Journal of Theoretical Biology*, *32*(3), 471–494. https://doi.org/10.1016/0022-5193(71)90152-4.

[8] J. Bajaj, G. Subba Rao, J. Subba Rao & R. Khardori (1987). A mathematical model for insulin kinetics and its application to protein-deficient (malnutrition-related) diabetes mellitus (PDDM). *Journal of Theoretical Biology*, *126*(4), 491–503. https://doi.org/10.1016/S0022-5193(87)80154-6.

[9] M. Chuedoung, W. Sarika & Y. Lenbury (2009). Dynamical analysis of a nonlinear model for glucose-insulin system incorporating delays and β-cells compartment. *Nonlinear Analysis-theory Methods Applications*, *71*(12), 1048–1058. https://doi.org/10.1016/j.na.2009.01.129.

[10] M. F. Faraloya, S. Shafie, F. M. Siam, R. Mahmud & S. O. Ajadi (2021). Numerical simulation and optimization of radiotherapy cancer treatments using the Caputo fractional derivative. *Malaysian Journal of Mathematical Sciences*, *15*(2), 161–187.

[11] A. Hurwitz (1964). On the conditions under which an equation has only roots with negative real parts. *Selected papers on mathematical trends in control theory*, *65*, 273–284.

[12] J. G. Liu & M. Y. Xu (2008). Study on the viscoelasticity of cancellous bone based on higher-order fractional models. *2008 2nd International Conference on Bioinformatics and Biomedical Engineering*, pp. 1733–1736. https://doi.org/10.1109/ICBBE.2008.761.

[13] Z. Odibat & N. Shawagfeh (2007). Generalized taylor's formula. *Applied Mathematics and Computation*, *186*(1), 286–293. https://doi.org/10.1016/j.amc.2006.07.102.

[14] Z. Odibat & S. Momani (2008). An algorithm for the numerical solution of differential equations of fractional order. *Journal of applied mathematics & informatics*, *26*(1-2), 15–27.

[15] G. Pacini & R. N. Bergman (1986). Minmod: a computer program to calculate insulin sensitivity and pancreatic responsivity from the frequently sampled intravenous glucose tolerance test. *Computer Methods and Programs in Biomedicine*, *23*(2), 113–122. https://doi.org/10.1016/0169-2607(86)90106-9.

[16] I. Podlubny (1999). *Fractional Differential Equations*. Academic Press, New York.

[17] S. Saber & A. Alalyani (2022). Stability analysis and numerical simulations of IVGTT glucose-insulin interaction models with two time delays. *Mathematical Modelling and Analysis*, *27*(3), 383–407. https://doi.org/10.3846/mma.2022.14007.

[18] S. Saber & S. M. Alzahrani (2019). Hopf bifurcation on fractional ordered glucose-insulin system with time-delay. *Albaha University Journal of Basic and Applied Sciences*, *3*(2), 27–34.

[19] S. Sayed, B. Eihab, S. Alzahrani & I. Noaman (2018). A mathematical model of glucose-insulin interaction with time delay. *Journal of Applied Computational Mathematics*, *7*(3), 417. https://doi.org/10.4172/2168-9679.1000416.

[20] A. R. Seadawy (2014). Stability analysis for Zakharov-Kuznetsov equation of weakly nonlinear ion-acoustic waves in a plasma. *Computers & Mathematics with Applications*, *67*(1), 172–180. https://doi.org/10.1016/j.camwa.2013.11.001.

[21] U. Younas, M. Younis, A. R. Seadawy, S. Rizvi, S. Althobaiti & S. Sayed (2021). Diverse exact solutions for modified nonlinear Schrodinger equation with conformable fractional derivative. *Results in Physics*, *20*, 103766. https://doi.org/10.1016/j.rinp.2020.103766.